Naval Research Laboratory

AD-A198 361

Stochastic Electron Detrapping in FELs Caused by Sidebands

S. RIYOPOULOS* AND C. M. TANG

*Science Applications Intl. Corp.,
McLean, VA 22102

Plasma Theory Branch
Plasma Physics Division

July 14, 1988

DTIC
ELECTE
SEP 1 5 1988
E

88 9 14 205

REPORT DOCUMENTATION PAGE

Form Approved
OMB No. 0704-0188

1a REPORT SECURITY CLASSIFICATION	1b RESTRICTIVE MARKINGS
UNCLASSIFIED	

2a SECURITY CLASSIFICATION AUTHORITY	3 DISTRIBUTION / AVAILABILITY OF REPORT
	Approved for public release; distribution
2b DECLASSIFICATION / DOWNGRADING SCHEDULE	unlimited.

4 PERFORMING ORGANIZATION REPORT NUMBER(S)	5 MONITORING ORGANIZATION REPORT NUMBER(S)
NRL Memorandum Report 6224	

6a NAME OF PERFORMING ORGANIZATION	6b OFFICE SYMBOL (If applicable)	7a NAME OF MONITORING ORGANIZATION
Naval Research Laboratory	Code 4790	U.S. Army Strategic Defense Command

6c ADDRESS (City, State, and ZIP Code)	7b ADDRESS (City, State, and ZIP Code)
Washington, DC 20375-5000	Arlington, VA 22245-0280

8a NAME OF FUNDING / SPONSORING ORGANIZATION Strategic Defense Initiative Org.	8b OFFICE SYMBOL (If applicable)	9 PROCUREMENT INSTRUMENT IDENTIFICATION NUMBER

8c ADDRESS (City, State, and ZIP Code)	10 SOURCE OF FUNDING NUMBERS			
	PROGRAM ELEMENT NO	PROJECT NO	TASK NO	WORK UNIT ACCESSION NO
Washington, DC 20301-7100	63221C	W31RPD-7-D4039		

11 TITLE (Include Security Classification)

Stochastic Electron Detrapping in FELs Caused by Sidebands

12 PERSONAL AUTHOR(S)
Riyopoulos,* S. and Tang, C.M.

13a TYPE OF REPORT	13b TIME COVERED	14 DATE OF REPORT (Year, Month, Day)	15 PAGE COUNT
Interim	FROM ___ TO ___	1988 July 14	51

16 SUPPLEMENTARY NOTATION
*Science Applications Intl. Corporation, McLean, VA 22102

17	COSATI CODES		18 SUBJECT TERMS (Continue on reverse if necessary and identify by block number)
FIELD	GROUP	SUB-GROUP	FELs Electron detrapping
			Sidebands Efficiency
			Stochasticity

19 ABSTRACT (Continue on reverse if necessary and identify by block number)

The growth of sidebands in an FEL above a certain threshold will result in stochastic electron motion. This may lead to significant electron detrapping and loss of amplification for the radiation field. The threshold in the sideband amplitude for the stochastic transition is computed. The rate trapped electrons leak outside the sepratrix is measured by the diffusion coefficient in action space. This approach is general and covers both tapered and untapered wigglers. Three general types of spectra are examined: a narrow, a broad discrete and a broad continuous. Each type is associated with a particular scaling of the diffusion coefficient on the FEL parameters. Numerical results, obtained for constant radiation amplitudes, show good agreement with the theoretical predictions. The diffusion rate is always proportional to the total sideband-to-carrier power ratio, with different coefficients of proportionality for each spectral type. The narrow types of sepctrum causes the ~

(Continues)

20 DISTRIBUTION / AVAILABILITY OF ABSTRACT	21 ABSTRACT SECURITY CLASSIFICATION
☒ UNCLASSIFIED/UNLIMITED ☐ SAME AS RPT ☐ DTIC USERS	UNCLASSIFIED

22a NAME OF RESPONSIBLE INDIVIDUAL	22b TELEPHONE (Include Area Code)	22c OFFICE SYMBOL
C.M. Tang	(202) 767-4248	Code 4790

DD Form 1473, JUN 86   Previous editions are obsolete   SECURITY CLASSIFICATION OF THIS PAGE

S/N 0102-LF-014-6603

i

19. ABSTRACTS (Continued)

highest diffusion rates and the broad continuous spectrum causes the lowest diffusion rates under constant total sideband power. The diffusion length, measured in wiggler periods, is independent of the beam energy γ. Serious deterioration in the FEL efficiency will result when the diffusion length becomes shorter than the wiggler length.

DD Form 1473, JUN 86 (Reverse)

CONTENTS

Accession For

NTIS GRA&I

DTIC TAB

Unannounced

Justification

By

Distribution/

Availability Codes

Dist   Avail and/or
        Special

A-1

DTIC
COPY
INSPECTED
2

STOCHASTIC ELECTRON DETRAPPING IN FELS
CAUSED BY SIDEBANDS

I. INTRODUCTION

Multifrequency effects in free electron lasers (FEL) become increasingly important as progress is made towards high power operation. Growth of parasitic frequencies (sidebands[1-5]) has been predicted theoretically and has been observed in experiments[6,7] as well as in simulations[8-10] with either constant or tapered wigglers[10]. The efficiency for the carrier signal is reduced and the optical quality is degraded as power is channeled into frequencies apart from the intented operation frequency. Another potential hazard that has attracted little attention so far is the onset of chaotic electron motion caused even by the presence of a single frequency sideband. This may lead to extensive particle detrapping and premature loss of the amplification for all the radiation modes independent of frequency.

So far the attention has been directed to the linear stability issue. The gain for small sideband signal has been computed analytically[1-5] invoking either ensemble averaging over single particle trajectories or solutions of the perturbed kinetic equation for the distribution function. Initial results, obtained for particles localized near the bottom of the ponderomotive well, and, in particular, more recent results including all trapped and untrapped particles[2] with arbitrary distributions, have made it clear that every nontrivial distribution $df_o/dJ \neq 0$ is unstable to sideband growth.

Given that sidebands cannot be eliminated, the growth of the unstable modes to a finite amplitude may have serious effects on the

unperturbed trajectories. It has been known that stochastic behavior[11] is an intrinsic property of perturbed Hamiltonian systems[12]. Accordingly the electron motion in an FEL will become chaotic when the sideband amplitude exceeds a certain threshold. This, in turn, will result into electron detrapping and potential loss of amplification for the electromagnetic fields.

In the present work we investigate the nonlinear effects caused by sidebands. The threshold for stochasticity, above which unbound chaotic motion occurs is determined. Once the stochastic transition takes place, the action J, a constant of motion in the unperurbed system, changes in a random manner. The ensamble average $\langle \Delta X^2 \rangle$ of any physical quantity X is described by a diffusion equation. Diffusion of the action invariant provides a measure of the leakage rate across the separatrix. If D is the effective diffusion coefficient in action space, then the diffusion length $L_d = J_s^2/D$ signifies the length over which approximately half of the deeply trapped particles get detrapped, where J_s is the action at the separatrix. We show that a single frequency sideband at one tenth (1/10) or less of the carrier amplitude suffices to spread irregular motion over most of the trapped particle domain. However, given that the interaction time of an electron in a FEL is short, we are mainly concerned on **how fast** this diffusion occurs. The diffusion rate increases and the diffusion length L_d decreases with increasing sideband amplitude(s). Thus a critical sideband level a_c can be defined above which the diffusion length L_d becomes shorter than the wiggler length L_w. Obviously the power level for the sidebands in a FEL

must not exceed a_c, otherwise extensive diffusion and premature detrapping will occur. On the other hand enough electrons can remain trapped during the interaction period even though their motion has turned stochastic when the critical amplitude a_c is much larger than the threshold for stochasticity α_s.

A clear-cut relation between the diffusion rate under constant total sideband power and the type of the excited sideband spectrum is discovered. More specifically we observe three regimes in the simulation parameters defining the sideband spectrum, corresponding to a narrow, a wide discrete and a wide continuous spectrum. The transition from one spectral type to another is accompanied by an abrupt change in the diffusion rates. In all cases we find the diffusion coefficient proportional to the ratio of the total power in the sidebands to the FEL carrier power. The coefficients of this proportionality depend on the spectral type. A general conclusion is that the diffusion rate, under constant sideband over carrier power ratio, decreases with increasing number of spectral components. The diffusion rate for a single sideband frequency exceeds that of a broad continuous spectrum by orders of magnitude while a broad discrete spectrum causes intermediate diffusion rates.

The analysis also shows that the normalized diffusion coefficient does not depend on the beam energy γ_r. The numerical results agree well with the theory.

II. TRANSITION TO STOCHASTICITY

We consider relativistic electrons streaming along the z-direction through the periodic magnetic wiggler and the radiation fields of the carrier and the sideband. We assume a circularly polarized static wiggler and constant amplitude electromagnetic waves. We assume that all waves propagate with the speed of light c, ignoring the small correction of order ω_p^2/ω_r^2 from the dielectric contribution of the beam. Electrostatic contributions to the fields are neglected for operation in the Compton regime. Both the wavenumber $k_w(z)$ and the amplitude $A_w(z)$ of the wiggler may change slowly in z on a scale length much longer than the wiggler wavelength $2\pi/k_w$. The FEL main signal wavenumber k_r is doubly Doppler upshifted from the wiggler wavenumber k_w,

$$k_r = 2\gamma_z^2 k_w , \tag{1}$$

with the upshifting factor $\gamma_z = (1 - \beta_r^2)^{-1/2}$ and $\beta_r = \omega_r/c(k_r + k_w)$.

We normalize the time t to ω_r^{-1}, the length z to k_r^{-1}, the mass to m_e and the vector potentials according to $a_i = |e|A_i/m_e c^2$ where the subscripts w, r, and s stand for wiggler, carrier and sideband respectively. The dimensionless Hamiltonian describing the electron motion for small deviations $\tilde{\gamma} = \gamma - \gamma_r$ from the resonant energy γ_r is given by,

$$H(\tilde{\gamma}, \psi; z) = \frac{k_w}{\gamma_r} \tilde{\gamma}^2 + \frac{a_w a_r}{\gamma_r}(\cos\psi + \psi \sin\psi_r) + \frac{a_w a_s}{\gamma_r}\cos(\psi - \delta_s z), \tag{2}$$

4

where ψ_r and δ_s are defined by,

$$\frac{d}{dz}\gamma_r = -\frac{k_r a_w a_r}{\gamma_r}\sin\psi_r \ , \qquad \delta_s = \frac{k_w}{k_r}\left(k_s - k_r\right), \tag{3}$$

The electron motion is parametrized by the traveled length z inside the wiggler. The term $\sin\psi_r$ parametrizes the rate of change for the resonant energy caused by the change in the wiggler wavelength where $\psi_r=0$ corresponds to an untapered wiggler. The term δ_s in the sideband phase is the Doppler downshifted difference between the signal and the sideband wavenumbers.

In the absence of sidebands, $a_s=0$, the Hamiltonian H_0 is integrable. The unperturbed trajectories in the ponderomotive well are given by $H_0(\tilde\gamma,\psi) = K$ where K is the reduced energy in the ponderomotive frame. These orbits take the simplest possible form expressed in terms of the action-angle variables (J, θ), defined as:

$$J = \frac{1}{2\pi}\oint d\psi\ \tilde\gamma(K,\psi), \qquad\qquad \theta = \frac{\partial}{\partial J}\int^{\psi}d\psi'\ \tilde\gamma(K,\psi')\ , \tag{4}$$

where $K = H_0(J)$ and the path of integration is over the unperturbed orbits. Hamiltonian (2) is transformed under the canonical transformation defined by Eq. (4) into,

$$H(J,\theta;z) = \tilde H_0(J) + \frac{a_w a_s}{\gamma_r}\sum_{n=0}^{\infty} Q_n^+(J)\cos(n\theta + \delta_s z) + Q_n^-(J)\cos(n\theta - \delta_s z), \tag{5}$$

$Q_n^+(J)$ are the Fourier coefficients obtained by the decomposition of the

perturbing sideband phase $\psi(J,\theta) - \delta_s z$ into harmonics of the angle θ, where $\psi(J, \theta)$ is obtained by inverting Eq. (4). In case of constant parameter wiggler J, θ and $Q_n(J)$ are expressed in closed forms given in Ref. 11.

$H_o(J)$ is independent of θ so the unperturbed orbits in (J, θ) space are straight lines $J = $ constant, $\theta = \theta_o + \kappa_b(J)z$. The synchrotron wavenumber $\kappa_b(J)$ is connected to the bounce length L_b and the synchrotron frequency in the laboratory frame $\omega_b(J)$ with the relation

$$\kappa_b(J) = \frac{dH_o(J)}{dJ} = \frac{2\pi}{L_b(J)} = \frac{\omega_b(J)}{c\beta_z} . \tag{6}$$

According to Eq. (5) new resonances emerge when a sideband is turned on. Defining the phase of the nth sideband induced harmonic $\Theta^{(n)} = n\theta \pm \delta_s z$, the stationary phase condition reads,

$$\pm n\kappa_b(J) - \delta_s = 0, \qquad \text{or} \qquad \pm n\beta_z\omega_b(J) - \delta_s = 0. \tag{7}$$

Thus particles, originally in unperturbed orbits $J = J_n$, resonate with the sideband when the nth harmonic of their synchrotron period $\omega_b(J_n)$ matches the downshifted frequency difference between the sideband and the carrier signal. When the sideband amplitude becomes finite these resonant particles get trapped inside secondary ponderomotive wells corresponding to the different harmonics in Hamiltonian (4). Thus a single frequency sideband causes chains of secondary islands to appear

6

inside the original primary island. The structure of the phase space is shown in Figs. 1a – 1d. They are surfaces of section, created by numerically integrating the original equations of motion from Hamiltonian Eq. (2) and then recording the intersection point of each trajectory with the plane $z = 2\pi/\delta_s$. The γ, ψ coordinates are plotted on the left side in Figs. 1a-1d. The plots on the right side show the same surfaces of section in action-angle variables, produced by the transformations (4).

The presence of just one sideband frequency suffices to transform the regular coherent motion, such as in Figs. 1a and 1c, to the irregular unbounded motion shown in Figs. 1b and 1d when the sideband amplitude exceeds a certain amplitude α_s regarded as the stochasticity threshold. The mechanism for this radical change in behavior can be briefly described as follows. The trajectories emanating from the unstable fixed points (X-points) of a secondary island corresponding to a given harmonic n do not actually join smoothly around that island. They intersect infinite times with each other[11,12] due to the effect of the other harmonics n' ≠ n, creating a thin layer of fussy motion that surrounds each island chain. As the amplitude a_s increases the width of each island increases and so does the thickness of the stochastic layer around that island. At a given point the stochastic layers around the two neighboring island chains n and n+1 overlap[13], allowing particles to hop from one island to another. This signifies the beginning of unbounded, random motion in J characterized as stochastic diffusion.

The overlapping condition that defines the transition to stochasticity is usually expressed by[11,13]

$$\delta J_n + \delta J_{n+1} \geq \frac{2}{3} \Delta J_n , \tag{8}$$

where δJ_n, δJ_{n+1} are the separatrix half-widths and $\Delta J_n = J_{n+1} - J_n$ is the distance between the separatrix centers for the n and n+1 harmonics respectively. δJ_n and ΔJ_n are evaluated from Hamiltonian (5) using the familiar methods of nonlinear dynamics in terms of the sideband amplitude a_s and the shear $d\kappa_b(J)/dJ$. The detailed computation, performed in Ref. 14, shows that the threshold for stochasticity α_s depends primarily on the frequency separation $(\omega_s - \omega_r)/\omega_r$ and less on the other FEL parameters. The ratio α_s/a_r varies in a semioscillatory manner between typical values of 0.1 and 1. The above threshold was derived for a single sideband frequency. Multifrequency sideband spectra generally tend to reduce α_s.

III. NARROW SPECTRUM DIFFUSION

We examine first the diffusion caused by a narrow sideband spectrum, meaning that the width of the sideband spectral line is much less than its distance from the carrier frequency. We model this case by a single frequency sideband. Figures 1b and 1d show a typical phase portrait when the sideband amplitude a_s is slightly above α_s. Two different kinds of regions coexist: a stochastic regime where diffusive

8

behavior prevails, interrupted here and there by islands of regular motion, remnants of the original regular motion. The stochastic regimes are interconnected allowing particle transport, hence α_s was defined as global stochasticity threshold.

Figure 2 illustrates the stochastic transition by plotting selected particle trajectories $J(z)$ with z measured in wiggler periods. The sideband amplitude increases from well below α_s in Fig. 2a to well above α_s in Fig. 2c. The initial conditions for the particles remain the same in all cases. The oscillations in Fig. 2a have the period of a particle trapped around a secondary island.

When a_s is increased well above α_s the chaotic motion engulfs almost 100% of the phase space. Total stochastization of the island interior occurs roughly when the sideband amplitude grows to the point where the stable fixed point $\tilde{\gamma} = 0$, $\psi = \pi + \psi_r$ at the centre of the original island becomes unstable.

The two questions of practical interest are: (a) what percentage of the particles will eventually get detrapped and (b) how fast do they leak outside the separatrix. For our uniform initial distribution the maximum fraction of particles becoming detrapped equals the fraction of the inside the separatrix area that becomes chaotic. In Fig. 3a we plot the fraction f_d of the particles that cross the original separatrix J_s as a function of the traveled wiggler length for values of a_s/a_r below the threshold for extended stochasticity. In all cases an initial stage of quick diffusion is followed by a long period where the average number of untrapped particles remains practically constant. The results are

consistent with the existence of a boundary in phase space (KAM surface) separating two regimes: the one of unbounded, chaotic motion from the one filled with regular, coherent orbits of particles that remain trapped. Only electrons in the area between the last integrable surface and the old unperturbed separatrix will diffuse until that area is depleted. A fraction $1 - f_d$ of the original primary island area will remain trapped for an arbitrarily long time, as long as a_s remains below the threshold α_s associated with the particular sideband frequency. This fraction is shrinking as a_s increases and the bucket "peels off". The situation when a_s exceeds α_s is shown in Fig. 3b. The fraction of untrapped particles f_d increases monotonically, reaching 1 in some cases, meaning complete absence of particle confinement in the bucket. All particles can eventually escape with a rate that increases with increasing a_s. The length over which approximately half of the initially trapped particles get detrapped will be discussed in the next section, in comparison with the diffusion rates from other types of sideband spectra. It is evident from the results in Fig. 3 that the diffusion length at constant amplitude a_s depends on the sideband frequency.

IV. BROAD FREQUENCY BAND DIFFUSION

So far stochastic electron detrapping caused by a single frequency sideband has been examined. Here, we consider the situation when many sideband frequencies have been excited. We will make a distinction between a continuous and a discrete spectrum. In case of a

discrete spectrum the distance between two nearby sideband frequencies is much larger than the width of an individual spectral line. In the opposite case when various peaks in the spectrum merge together we will talk about a continuous spectrum. We may model numerically both cases by introducing a modulation in the sideband phase of Hamiltonian Eq. (4),

$$H(\tilde{\gamma}, \psi; z) = \frac{k_w}{\gamma_r} \tilde{\gamma}^2 + \frac{a_w a_r}{\gamma_r}(\cos\psi + \psi \sin\psi_r) + \frac{a_w a_s}{\gamma_r}\cos(\psi + A \sin \nu z - \delta_s z),$$

(9)

that is transformed in action-angle variables as,

$$H(J, \theta; z) = H_0(J)$$

(10)

$$+ \frac{a_w a_s}{\gamma_r} \sum_{m=-\infty}^{\infty} J_m(A) \sum_{n=0}^{\infty} Q_n^+(J) \cos[n\theta + \delta_s(m)z] + Q_n^-(J) \cos[n\theta - \delta_s(m)z] .$$

The frequency mismatch values $\delta_s(m)$ and the corresponding sideband frequencies $\omega_s(m)$ are given by,

$$\delta_s(m) = \delta_0 + m \nu, \qquad \omega_s(m) = \omega_{so} + 2 m \gamma_z^2 \nu,$$

(11)

where $\omega_{so} = \omega_r + 2\gamma_z^2 \delta_0$. Since the Bessel function coefficients become vanishingly small, $J_m(A) \ll 1$ for $A > m$, the width of the spectrum is given by $D\delta_s \sim A \nu$ or $D\omega_s \simeq 2\gamma_z^2 A\nu$.

In order to examine the connection between diffusion rates and the types of the sideband spectra, we divide the latter into three

11

general categories: narrow, broad discrete and broad continuous. The passage from one regime to the other is characterized by abrupt changes in the diffusion coefficients. Both cases of the broad spectrum are characterized by a width $D\omega_s$ in the excited frequencies that is larger than the upshifted synchrotron frequency ω_b, $D\omega_s > 2\gamma_z^2\omega_b$, or equivalently,

$$\nu > \frac{\omega_b}{A} , \qquad (12)$$

with $A \gg 1$. The further distinction between discrete or continuous spectrum is related to the separation between nearby frequencies. We find that when $\omega_b/A^{1/2} > \nu > \omega_b/A$ the diffusion rate agrees well with the quasilinear diffusion coefficient. A different coefficient is derived for the case when $\nu > \omega_b/A^{1/2} > \omega_b/A$, in agreement with the numerical simulations. Consequently, the separation $\omega_b/A^{1/2}$ between nearby modes marks the transition from a discrete to a continuous type of behavior.

(a). Broad Discrete Spectrum.

We now evaluate the diffusion coefficient for a broad, discrete spectrum associated with frequency separation $\nu > \omega_b/A^{1/2}$. Due to the presence of many frequencies in the spectrum $J(z)$ executes a complicated oscillatory motion with the average $\langle J \rangle$ changing very little most of the time. J however receives a large kick ΔJ near resonances, where the

phase $\Phi = \psi + A \sin \nu z \pm \delta_s z$ of the multifrequency Hamiltonian (9)
varies slowly. The resonant condition is

$$\frac{d\Phi}{dz} = \frac{k_w \tilde{\gamma}}{\gamma_r} + A \nu \sin \nu z_i \pm \delta_s = 0, \qquad (13)$$

at some $z = z_i$. Given that $k_w \tilde{\gamma}/\gamma_r \lesssim \omega_b$, collective effects due to many
frequencies are important for the resonance in Eq. (13) when $A \nu > \omega_0$.
On this basis inequality (12) signifies the transition from a narrow to
a broad spectrum. Let us consider the case $A \nu \gg \omega_b$. Then the
resonances occur at $z_i \simeq i\pi/\nu$, i integer, and the interval between
successive resonances is $\Delta z \simeq \pi/\nu$. Expanding the phase $\Phi(z)$ in the
equation of motion for J around the resonance z_i, and extending the
limits of the z integration from $-\infty$ to $+\infty$ we obtain, for $A \nu^2 \gg \omega_b^2$,

$$DJ_i \simeq \frac{a_w a_r}{\gamma_r} \left(\frac{2\pi}{A \nu^2}\right)^{1/2} \cos\left(\Phi_n \pm \frac{\pi}{4}\right) |V(\psi_{mx}) - V(\psi_i)|^{1/2}, \qquad (14)$$

where $V(\psi) = \cos\psi + \psi \sin\psi_r$. The resonant phases Φ_i between two
successive jumps ΔJ become quickly decorrelated when a_s grows above the
stochasticity threshold. Assuming complete decorrelation in Φ_i between
two successive jumps we obtain,

$$D_w = \frac{2 \langle \Delta J^2 \rangle}{\Delta z} = \frac{2 a_w^2 a_s^2}{\gamma_r^2 A \nu}, \qquad (15)$$

where $\langle.... \rangle$ is the ensemble average over ψ_i, Φ_i. For practical purposes it is more convenient to rescale the diffusion coefficient so that the distance $\underline{z} = z/\lambda_w$ is measured in terms of wiggler wavelengths and the action $\underline{J} = J/J_s$ signifies the location relative to the separatrix. In these units, using Eq. (4) for J_s and setting $\nu / \omega_b(0) = r$ we obtain

$$\underline{D}_w = \frac{2\pi}{k_w} \frac{D_w}{J_s^2} = \frac{\pi^3}{8} \frac{g^2}{A\,r} \left(\frac{a_w a_r}{1 + a_w^2}\right)^{1/2} \frac{a_s^2}{a_r^2} . \tag{16}$$

The term g is a scaling factor, the ratio of the untapered wiggler separatrix to that of a tapered wiggler, depending only on ψ_r, $g = J_s(\psi_r=0)/J_s(\psi_r)$. The typical diffusion length L_d, the traveled distance inside the wiggler over which the average trapped particle crosses the separatrix is estimated from $\langle \Delta J^2 \rangle = J_s^2 = D_w L_d$. Thus, the diffusion length in wiggler periods $N_d = L_d/\lambda_w$ is the inverse of $\underline{D}_w$, $N_d = 1/\underline{D}_w$.

(b). Broad Continuous Spectrum

Next we consider the case of a sideband wave package,

$$a_s(z,t) = \frac{1}{2\pi} \int dk_s a_s(k_s) e^{ik_s z - i\omega(k_s)t} , \tag{17}$$

of finite spectral width Dk_s centered around k_{so}. Our purpose is to obtain the diffusion coefficient for a continuous spectrum using the methods of the quasilinear theory.

One condition for the applicability of the quasilinear theory is that the phase mixing due to Dk_s occurs much faster than the bounce period around a secondary island in phase space. This way electrons, that otherwise would execute periodic orbits around some fixed point, lose coherency fast enough and a random motion of the Fokker-Planck type sets in. This condition is satisfied for spectral widths Dk_s of order,

$$\frac{Dk_s}{k_s} \gg 2 \; \gamma_z^{\;2} \; \frac{\kappa_b^{\;2}(0)}{k_r^{\;2}} \; . \tag{18}$$

The overlapping condition among nearby island chains, similar to Eq. (8), must also be satisfied. The threshold for overlapping is much lower than α_s related to the single sideband frequency. Then the evolution of the initial distribution $f_0(J)$ is globally described by a diffusion equation,

$$\frac{\partial f}{\partial z} = \frac{\partial}{\partial J} \; D_q(J) \; \frac{\partial f}{\partial J} \; .$$

Applying the standard procedures of the quasilinear theory[15] and taking the limit of small growth rate for the sidebands, $\mathrm{Im}(k_s)/k_s \ll 1$, we obtain the quasilinear diffusion coefficient,

$$D_q(J) = \frac{k_r \; a_w^{\;2} \; \gamma_z^{\;2} \; W_s(k_{so}) \; k_w \; J}{\gamma_r^{\;3} \omega_b(J)} \; . \tag{19}$$

We express $D_q(J)$ in normalized units, with the wiggler wavelength λ_w as

the unit length and the action J_s at the separatrix as the unit action. Chosing the value $J = J_s/2$ inside $D_q(J)$ we obtain an estimate for the effective diffusion coefficient associated with the uniformly filled distribution,

$$D_q = \frac{2\pi}{k_w} \frac{D_q(J)}{J_s^2} \sim \frac{\pi}{4} \frac{g\, a_w a_r}{\Lambda\, (1+a_w^2)} \frac{W_s(t)}{Dk_s\, W_r(t)} , \qquad (20)$$

where g is the same scaling factor as in Eq. (16).

Note that both expressions (16) and (20) for D, corresponding to the two different spectral types, are independent of γ_r. Thus, for the same wiggler parameters and total sideband power, the detrapping distance in wiggler periods is independent of the electron beam energy.

A more detailed treatement of the subject, including the derivation of the formulas (16) and (20) is found in Ref. 14.

V. NUMERICAL RESULTS

The trajectories J(z) on the left side of 4a-4c are generated by the same initial conditions for the electrons, the same FEL parameters a_w, a_r and k_w, and the same averaged sideband power $\langle a_s^2 \rangle$. The spectral parameters A and ν however are different so that each of the cases (a) (b) and (c) corresponds to one of the three spectral types defined earlier. The dashed line marks the position of the unperturbed separatrix J_s. Without the sidebands the trajectories would be straight

16

lines. The corresponding distribution functions $f(J,z)$ are plotted on the right-hand side at the beginning, $z = 0$, halfway inside, $z = 50\lambda_w$, and at the end, $z = 100\lambda_w$ of the wiggler.

The numerically computed diffusion length in wiggler periods $N_d = 1/\underline{D}$ is plotted against the sideband to carrier power ratio $P = \sum_n a_s^2(\omega_n)/a_r^2 = W_s/W_r$ in Fig. 5 for the three different types of spectra . We have integrated numerically the equations of motion for 400 particles of a uniform initial distribution inside the bucket. The field intensities remained constant at $a_r = 5\times10^{-5}$, $a_w = 2$ and $\gamma_r = 25$. A clear separation in the diffusion rates is observed among the various spectral types. The narrow frequency results (triangles) were obtained using the Hamiltonian (2) with a single sideband frequency $\omega_s/\omega_r = 1.016$. The results for a broad discrete spectrum (circles) were obtained using (9) with $A = 20$, $\omega_s/\omega_r = 1.016$ and $\nu = 0.5\,\delta_s$. The continuous spectrum (squares) was modeled by $A = 100$, $\nu = 0.05\,\delta_s$. The solid lines correspond to the theoretical results of Eqs. (16) and (20), in good agreement with the numerics. Theoretical predictions for the single frequency case were not made. We stress however the difference between single frequency results and quasilinear theory in this case. The agreement that has been observed in some other cases is not generic but particular to certain systems.

Finally, in Fig. 6 we plot the diffusion coefficient for a uniformly filled bucket as a function of the energy γ_r, fixing the wiggler parameters. It is clear that the diffusion rate (measured again in number of wiggler periods) is independent of the beam energy,

17

provided the synchrotron frequency ω_b stays in the same parameter regime.

Once the diffusion coefficients are known some estimate can be made of the related reduction in efficiency over the wiggler length. Assuming that $n_b(z) = n_b(0) \exp(-z/L_d)$ the number of detrapped particles between z and $z + \Delta z$ is $\Delta n(z) = n_b(0)L_d^{-1} \exp(-z/L_d) \Delta z$. These particles gave up an amount of energy $\Delta E(z) = [\gamma_r(0) - \gamma_r(z)] \Delta n(z)$ as radiation. Integrating $\Delta E(z)$ over the wiggler length for a linearly tapered wiggler $\gamma_r(z) = \gamma_r(0) - \Delta\gamma \, z \, / \, L_w$ we find the total energy extracted from the particles that were detrapped at some point inside the wiggler. Adding the contribution $[\gamma_r(0) - \gamma_r(L_w)] \, n_b(L_w)$ from the particles that remained trapped throughout the wiggler length we come up with,

$$\eta(L_w) = \eta_o \frac{L_d}{L_w} \left(1 - \exp \left(- \frac{L_w}{L_d} \right) \right), \tag{21}$$

where $\eta_o = \Delta\gamma/\gamma_r(0)$ is the efficiency without induced diffusion. The loss of amplification will in general be distributed among all the radiation modes and (21) reflects the total power loss in all frequencies.

Acknowledgement

REFERENCES

1. N. M. Kroll, P. L. Morton and M. N. Rosenbluth in Free Electron Generators of Coherent Radiation, Vol. 7 (Addison-Wesley, Reading, MA) p. 147 (1980).

2. S. Riyopoulos and C. M. Tang, Proc. Eighth Intl. Conf. FELs, Glasgow, UK (North Holland, M. Poole, ed.) 226, (1987).

3 S. S. Yu, W. M. Sharp, W. M. Fawley, E. T. Scharlemann, A. M. Sessler and E. J. Sternbach, Proc. Eighth Intl. Conf. FELs, Glasgow, UK (North Holland, M. Poole, ed.) 219, (1987).

4. R. C. Davidson and J. S. Wurtele, Phys. Fluids 30, 557 (1987).

5. R. C. Davidson and J. S. Wurtele, Phys. Fluids 30, 2825 (1987).

6. T. Masud, T. C. Marshall, S. P. Schlesinger and F. G. Yee, Phys. Rev. Lett. 56, 1567 (1986).

7. T. Masud, T. C. Marshall, S. P. Schlesinger, F. G. Yee, W. M. Fawley, E. T. Scharlemann, S. S. Yu, A. M. Sessler and E. J. Sternbach, to be published.

8. C. M. Tang and P. Sprangle in Free Electron Generators of Coherent Radiation (S. F. Jacobs, M. O. Scully, eds.) SPIE 453, 11 (1983).

9. W. B. Colson, Proc. Seventh Intl. Conf. FELs (North Holland, E. T. Scharlemann, D. Prosnitz, eds.) p. 168 (1985); also W. B. Colson, Proc. Intl. Conf. Lasers (STS Press, McLean, VA) p. 751 (1982).

10. D. C. Quimby, J. M. Slater and J. P. Wilcoxon, IEEE J. Quant. El. 21, 979 (1986).

11. See, for example, A. J. Lichtenberg and M. A. Lieberman "Regular and Stochastic Motion" (Springer-Verlag, New York, 1983), and references therein.

12. H. Poincare, "New Methods of Celestial Mechanics", (Dover, New York, 1957).

13. B. V. Chirikov, Phys. Reports $\underline{52}$, 265 (1979)

14. S. Riyopoulos and C. M. Tang, submitted for publication to Phys. of Fluids.

15. A. Vedenov, E. Velikhov and R. Z. Sagdeev, Nucl. Fusion $\underline{1}$, 82 (1961); also W. E. Drummond and D. Pines, Nucl. Fusion, Suppl. 3, 1049 (1962).
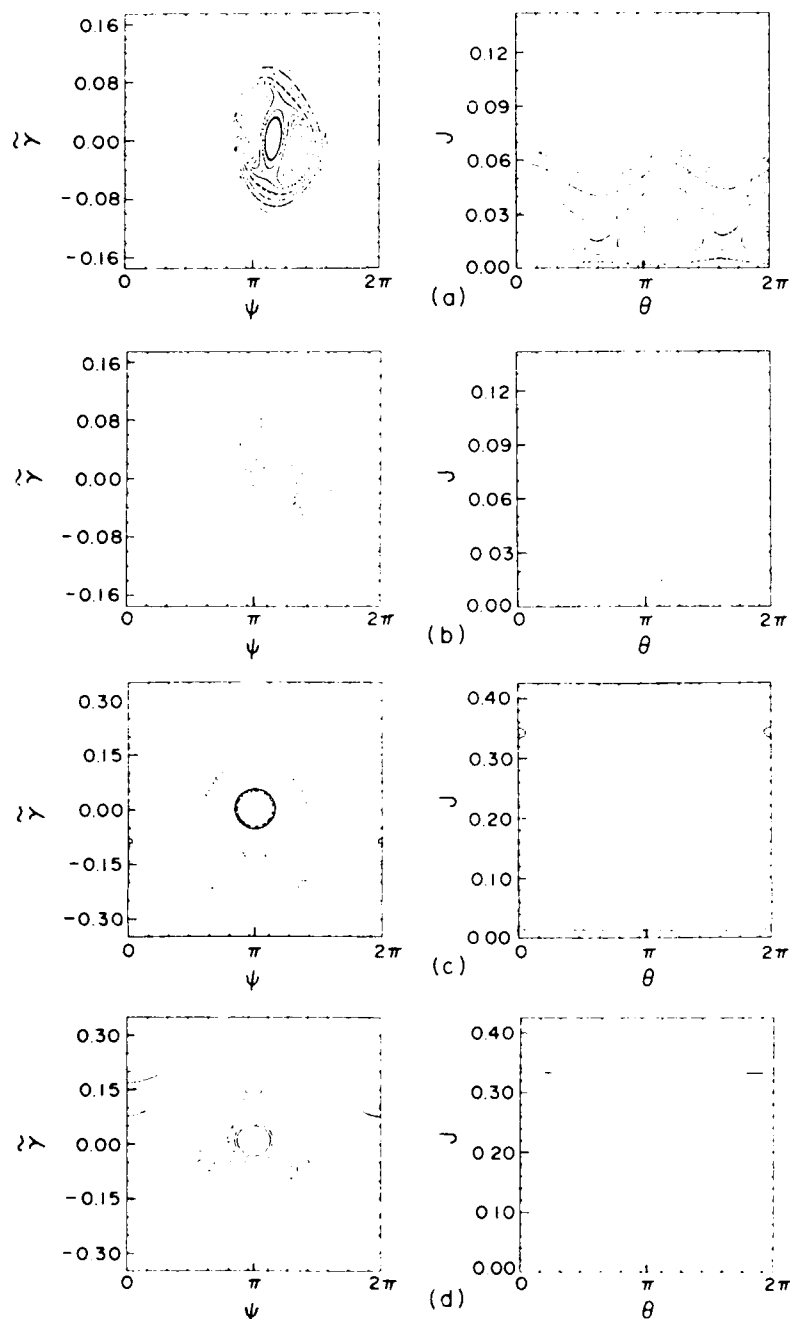
Figure 1. Plots of surfaces of section in both $\tilde{\gamma}$, ψ and J, θ representations, illustrating transition to chaotic behavior. The parameters are $a_w = 2$, $a_r = 5\times10^{-5}$ and initial $\gamma_r = 25$. Figures (a) and (b) correspond to tapered wiggler, $\psi_r = 4\pi/3$, with $\omega_s/\omega_r = 1.016$ and (a) $a_s = 2\times10^{-6}$, (b) $a_s = 1\times10^{-5}$. Figures (c) and (d) correspond to untapered wiggler with $\omega_s/\omega_r = 1.024$ and (c) $a_s = 2\times10^{-6}$, (d) $a_s = 1\times10^{-5}$.
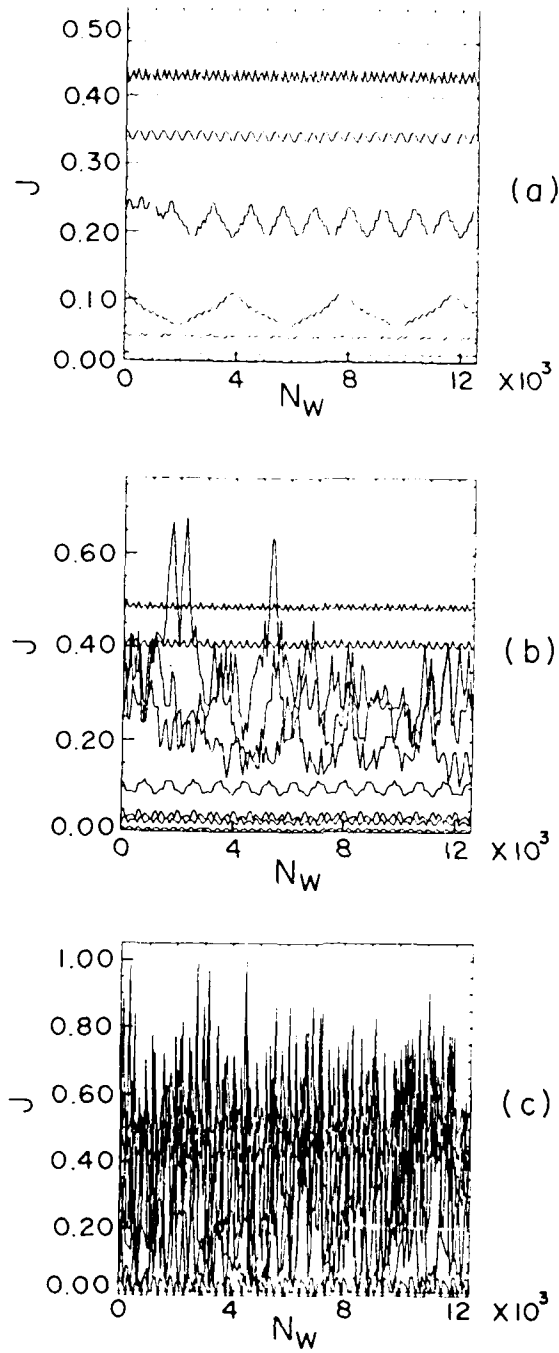
Figure 2.   Transition to chaotic behavior. The action J is plotted against the number of wiggler periods N_w. The parameters are $a_w = 2$, $a_r = 5 \times 10^{-5}$, $\gamma_r = 25$, $\omega_s/\omega_r = 1.024$ and (a) $a_s = 2 \times 10^{-6}$, (b) $a_s = 1 \times 10^{-5}$ and (c) $a_s = 5 \times 10^{-5}$.
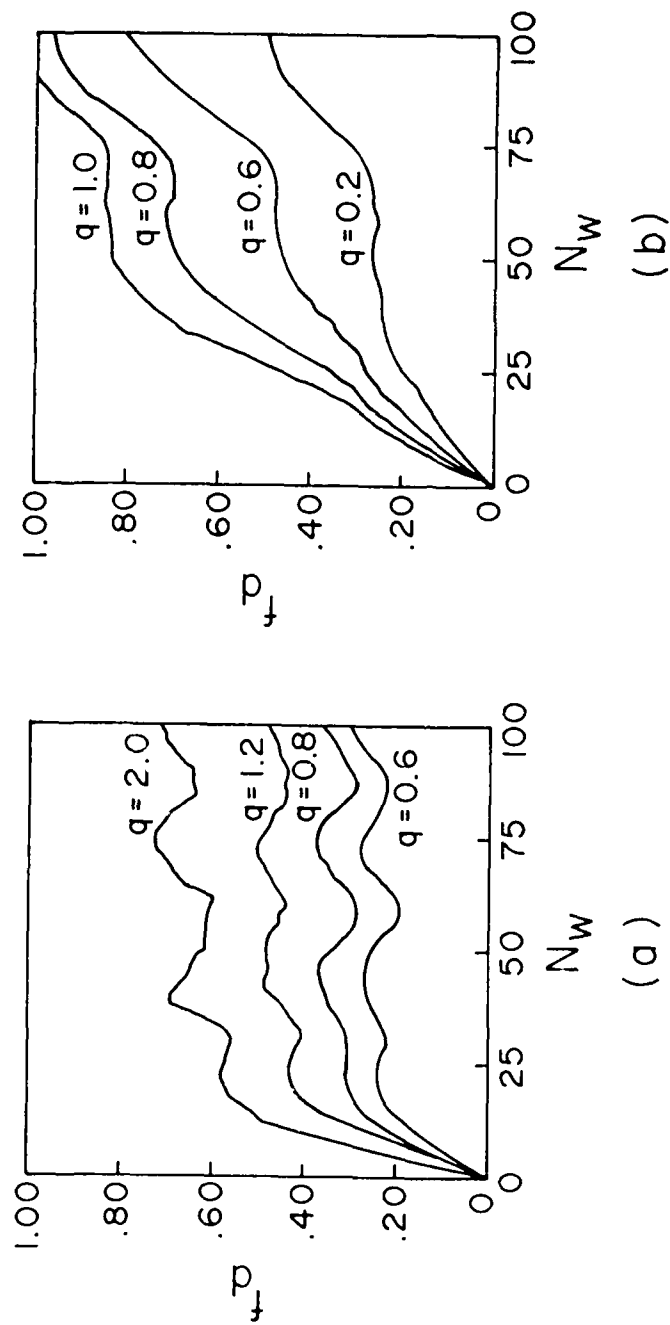
Figure 3.   The fraction f_d of detrapped particles against the distance in wiggler periods $N_w = z / \lambda_w$. Different curves correspond to various sideband to carrier amplitude ratios $q = a_s/a_r$. Parameters are $a_w = 2$, $a_r = 5 \times 10^{-5}$, $\gamma_r = 25$ and (a) $\omega_s/\omega_r = 1.016$, (b) $\omega_s/\omega_r = 1.024$.

23
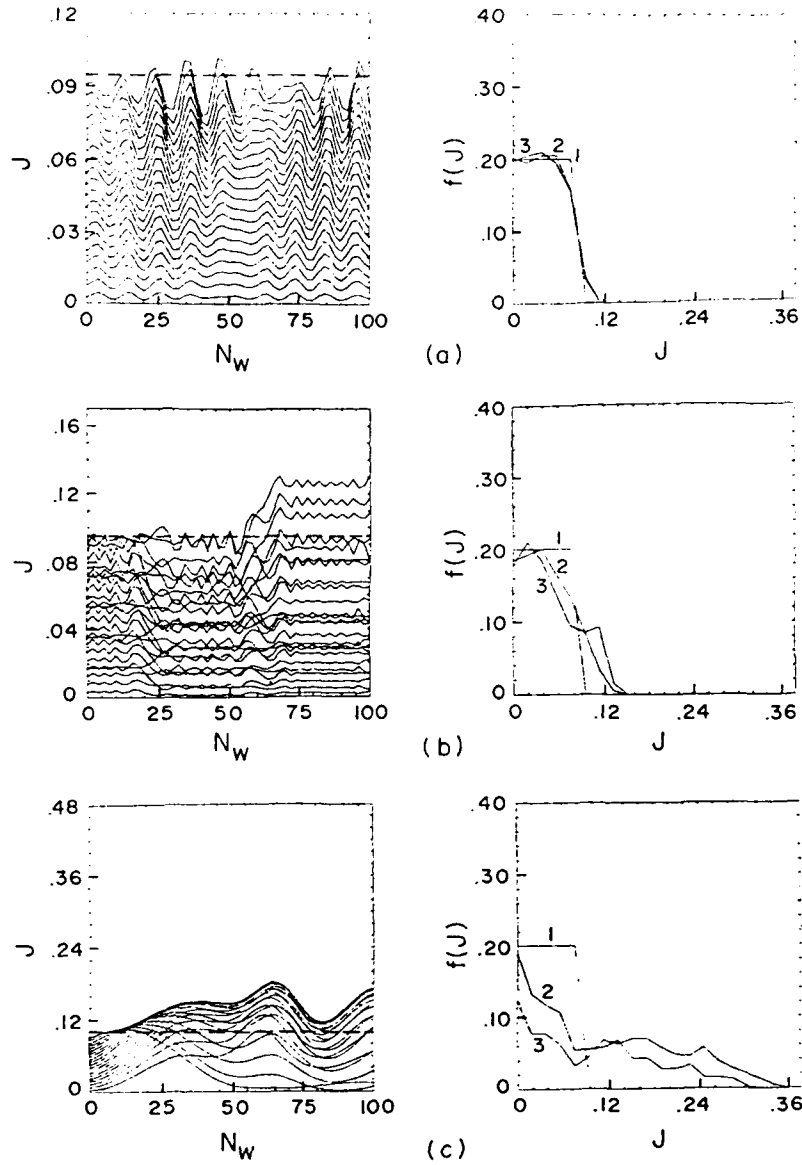
Figure 4. Particle response under different sideband spectra. On the left-hand side we plot the action J against the number of wiggler periods N_w for selected particles. On the right-hand side we plot the corresponding distribution function $f(J)$ at $N_w = 0$, 50, and 100. In all cases the total sideband fractional power $P = W_s/W_r = 0.36$ and $a_w = 2$, $a_r = 5 \times 10^{-5}$, $\gamma_r = 25$. (a) corresponds to a discrete sideband spectrum with $\omega_s/\omega_r = 1.016$. (b) corresponds to a wide discrete spectrum and (c) to a wide continuous spectrum.

24
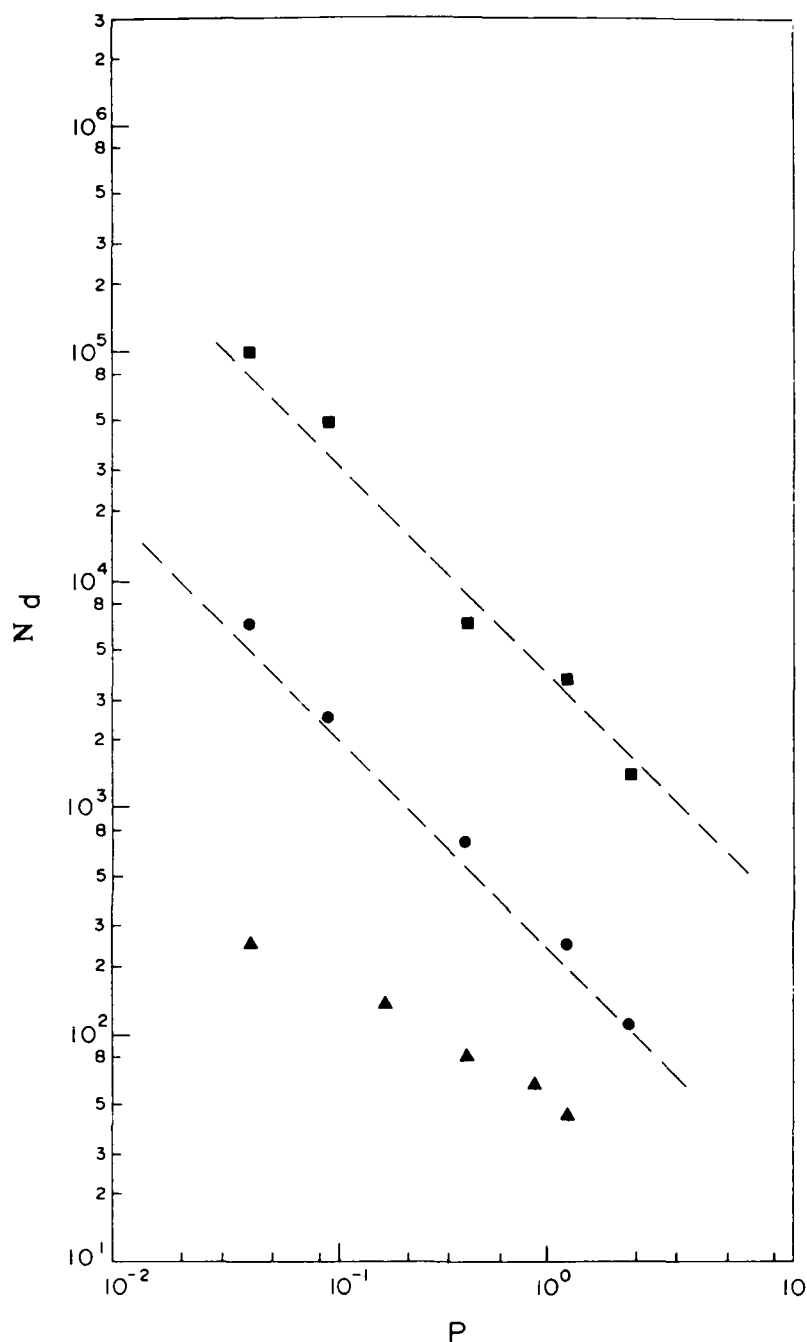
Figure 5. The e-folding diffusion length $N_d = 1/D$ as a function of the sideband fractional power $P = W_s/W_r$ for $a_w = 2$, $a_r = 5 \times 10^{-5}$, $\gamma_r = 25$ and $\omega_s/\omega_r = 1.016$. Squares correspond to a continuous, dots to a wide discrete and triangles to a single frequency spectrum. The upper and lower solid lines correspond to the theoretical results Eqs. (16) and (20) respectively.
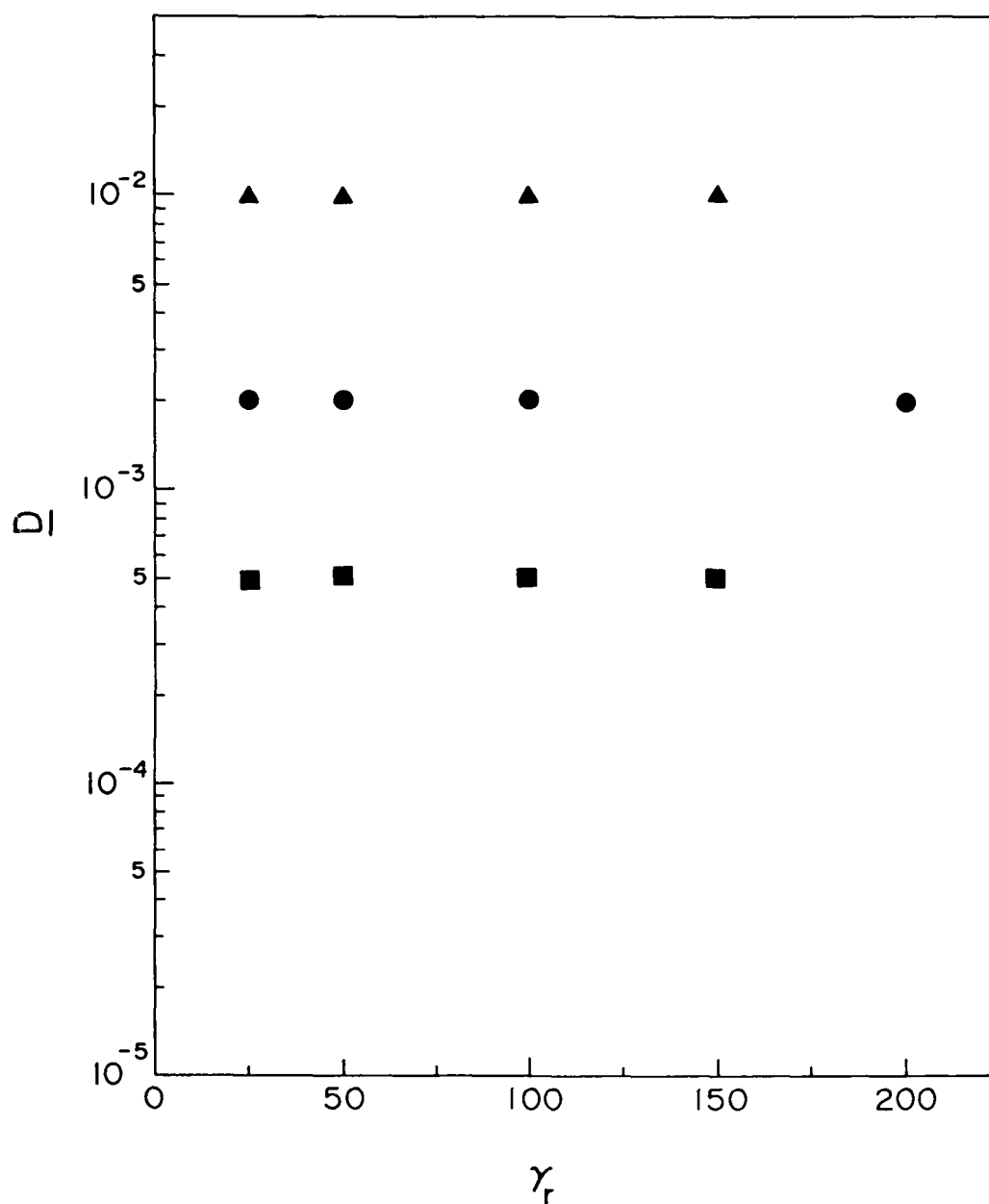
Figure 6.   Plots of the normalized diffusion coefficient $\underline{D}$ against the electron energy γ_r for $a_w = 2$, $a_r = 2\times10^{-4}$ and $a_s = 7.5\times10^{-5}$. Squares correspond to a continuous, dots to a wide discrete and triangles to a single frequency spectrum.

DISTRIBUTION LIST*

Naval Research Laboratory
4555 Overlook Avenue, S.W.
Washington, DC 20375-5000

    Attn: Code 1000 - Commanding Officer, CAPT W. G. Clautice
                1001 - Dr. T. Coffey
                1005 - Head, Office of Management & Admin.
                1200 - CAPT M. A. Howard
                1220 - Mr. M. Ferguson
                2000 - Director of Technical Services
                2604 - NRL Historian
                4000 - Dr. W. R. Ellis
                4600 - Dr. D. Nagel
                4603 - Dr. W. W. Zachary
                4700 - Dr. S. Ossakow (26 copies)
                4700.1-Dr A. W. Ali
                4710 - Dr. C. A. Kapetanakos
                4730 - Dr. R. Elton
                4740 - Dr. W. M. Manheimer
                4740 - Dr. W. Black
                4740 - Dr. J. Condon
                4740 - Dr. A. W. Fliflet
                4740 - Dr. S. Gold
                4740 - Dr. D. L. Hardesty
                4740 - Dr. A. K. Kinkead
                4740 - Dr. M. Rhinewine
                4770 - Dr. G. Cooperstein
                4790 - Dr. P. Sprangle
                4790 - Dr. C. M. Tang (50 copies)
                4790 - Dr. M. Lampe
                4790 - Dr. Y. Y. Lau
                4790A- W. Brizzi
                5700 - Dr. L. A. Cosby
                6840 - Dr. S. Y. Ahn
                6840 - Dr. A. Ganguly
                6840 - Dr. R. K. Parker
                6843 - Dr. R. H. Jackson
                6843 - Dr. N. R. Vanderplaats
                6875 - Dr. R. Wagner
                2628 - Documents (20 copies)
                2634 - D. Wilbanks

* Every name listed on distribution gets one copy except for those where
extra copies are noted.

27

Dr. R. E. Aamodt
Science Appl. Intl. Corp.
1515 Walnut Street
Boulder, CO 80302

Dr. J. Adamski
Boeing Aerospace Company
P.O. Box 3999
Seattle, WA 98124

Dr. H. Agravante
TRW, Inc.
One Space Park
Redondo Beach, CA   90278 / R1-2020

Prof. I. Alexeff
University of Tennessee
Dept. of Electrical Engr.
Knoxville, TN 37916

Dr. L. Altgilbers
3805 Jamestown
Huntsville, AL 35810

Dr. A. Amir
Quantum Inst. and Dept. of Physics
University of California
Santa Barbara, CA 93106

Dr. Bruce Anderson
Air Force Weapons Laboratory
Kirtland AFB
Albuquerque, NM 87117

Dr. Antonio Anselmo
909 Mitchell Street
Cornell University
Ithaca, NY 14850

Dr. T. M. Antonsen
University of Maryland
College Park, MD 20742

Dr. C. M. Armstrong
Code 6843
Naval Research Laboratory
Washington, DC 20375-5000

Dr. Tony Armstrong
Science Applications Intl. Corp.
P.O. Box 2351
La Jolla, CA 92038

Assistant Secretary of the
Air Force (RD&L)
Room 4E856, The Pentagon
Washington, D.C. 20330

Dr. W. P. Ballard
Sandia National Laboratories
ORG. 1231, P.O. Box 5800
Albuquerque, NM 87185

Mr. Jon Barber
Dept. of Physics
Bethel College
St. Paul, MN 55112

Dr. W. A. Barletta
Lawrence Livermore National Lab.
P. O. Box 808
Livermore, CA 94550

Dr. L. R. Barnett
3053 Merrill Eng. Bldg.
University of Utah
Salt Lake City UT 84112

Commander George Bates, PMS 405-300
Naval Sea Systems Command
Department of the Navy
Washington, DC 20362

Dr. Latika Becker
U. S. Army SDC
DASD-H-F
P. O. Box 1500
Huntsville, AL 35807-3801

Dr. W. Becker
Univ. of New Mexico
Institute for Mod. Opt.
Albuquerque, NM 87131

Dr. Robert Behringer
Code 818
Office of Naval Research
1030 E. Green
Pasadena, CA 91106

Dr. G. Bekefi (5 copies)
Mass. Institute of Tech.
Bldg. 26
Cambridge, MA 02139

Dr. S. Bender
Los Alamos National Laboratory
P. O. Box 1663
Los Alamos, NM 87545

Dr. J. Benford
Physics International
2700 Merced Street
San Leandro, CA 94577

Dr. Herbert S. Bennett
National Bureau of Standards
Bldg. 225, Rm. A352
Washington, DC 20234

Dr. S. Benson
S.P.R.C.
Dept. of Physics
Stanford University
Stanford, CA 94305

Dr. T. Berlincourt
Office of Naval Research
Attn: Code 420
Arlington, VA 22217

Dr. I. B. Bernstein (10 copies)
Mason Laboratory
Yale University
400 Temple Street
New Haven, CT 06520

Dr. Vladislav Bevc
Synergy Research Institute
P.O. Box 561
San Ramon, CA 94583

Dr. Anup Bhowmik
Rockwell International/Rocketdyne Div.
6633 Canoga Avenue, FA-40
Canoga Park, CA 91304

Dr. K. Jim Bickford
RDA
2301F Yale Blvd., S.E.
Albuquerque, NM 87106

Dr. D. L. Birx
Lawrence Livermore National Laboratory
P. O. Box 808
Livermore, CA 94550

Dr. J. Bisognano
Lawrence Berkeley Laboratory
University of California, Berkeley
Berkeley, CA 94720

Dr. Steve Bitterly
Rockwell International/Rocketdyne Div.
6633 Canoga Avenue, FA-40
Canoga Park, CA 91304

Dr. H. Boehmer
TRW DSSG
One Space Park
Redondo Beach, CA 90278

Dr. P. Bosco
KMS Fusion Inc.
Ann Arbor, MI 48106

Dr. I. Boscolo
Quantum Institute
University of California
Santa Barbara, CA 93106

Dr. B. Boswell
Lab for Laser Energetics
University of Rochester
250 E. River Road
Rochester, NY 14623

Dr. G. Bourianoff
1901 Rutland Drive
Austin, TX 78758

Dr. J. K. Boyd
Lawrence Livermore National Laboratory
P. O. Box 808
Livermore, CA 94550

Dr. H. Brandt
Department of the Army
Harry Diamond Laboratory
2800 Powder Mill Rd.
Adelphi, MD 20783

Dr. Charles Brau (2 copies)
Los Alamos National Laboratory
P.O. Box 1663, M.S. - 817
Los Alamos, NM 87545

Dr. R. Briggs
Lawrence Livermore National Lab.
Attn: (L-71)
P.O. Box 808
Livermore, CA 94550

Dr. D. L. Bullock
Optical Sciences Department
TRW Space and Technology Group
Redondo Beach, CA 90278

Dr. Art Chester
Hughes E51
Mail Stop A269
P.O. Box 902
El Segundo, CA 90245

Dr. Abraham Chian
IGPD
Univ. of Calif. at Los Angeles
Los Angeles, CA 90024

Dr. S. C. Chiu
GA Technologies Inc.
P.O. Box 85608
San Diego, CA 92138

Dr. Y. C. Cho
NASA-Lewis Research Center
Mail Stop-54-5
Cleveland, Ohio 44135

Dr. J. Christiansen
Hughes Aircraft Co.
Electron Dynamics Division
3100 West Lomita Blvd.
Torrance, CA 90509

Dr. T. L. Churchill
Spectra Technology, Inc.
2755 Northup Way
Bellevue, WA 98004

Major Bart Clare
USASDC
P. O. BOX 15280
Arlington, VA 22215-0500

Dr. Melville Clark
8 Richard Road
Wayland, MA 01778

Dr. Robert Clark
P.O. Box 1925
Washington, D.C. 20013

Dr. David B. Cline
The Inst. for Accelerator Physics
Department of Physics
University of Wisconsin-Madison
Madison, WI 53706

Dr. Alan J. Cole
TRW
One Space Park
Redondo Beach, CA 90278

Dr. William Colson
Berkeley Research Asso.
P. O. Box 241
Berkeley, CA 94701

Dr. William Condell
Office of Naval Research
Attn: Code 421
800 N. Quincy St.
Arlington, VA 22217

Dr. Richard Cooper
Los Alamos National Scientific
Laboratory
P.O. Box 1663
Los Alamos, NM 87545

Dr. Robert S. Cooper
Director, DARPA
1400 Wilson Boulevard
Arlington, VA 22209

Dr. M. Cornacchia
Lawrence Berkeley Laboratory
University of California, Berkeley
Berkeley, CA 94720

Dr. R. A. Cover
Rockwell International/Rocketdyne Div.
6633 Canoga Avenue, FA-38
Canoga Park, CA 91304

Dr. D. Crandall
ER-55, GTN
Department of Energy
Washington, DC 20545

Dr. M. S. Curtin
KMS Fusion, Inc.
P.O. Box 1567
Ann Arbor, MI 48106

Dr. Antonello Cutolo
Research Associate
Hansen Labs
NEPL Annex
Stanford University
Stanford, CA 94305

Dr. Bruce Danly
MIT
NW16-174
Cambridge, MA 02139

Dr. A. England
Oak Ridge National Laboratory
P.O. Box Y
Mail Stop 3
Building 9201-2
Oak Ridge, TN 37830

Dr. William M. Fairbank
Phys. Dept. & High Energy
Phys. Laboratory
Stanford University
Stanford, CA 94305

Dr. Anne-Marie Fauchet
Brookhaven National Laboratories
Associated Universities, Inc.
Upton, L.I., NY 11973

Dr. J. Feinstein
Dept. of Electrical Engineering
Stanford University
Stanford, CA 94305

Dr. Frank S. Felber
11011 Torreyana Road
San Diego, CA 92121

Dr. D. Feldman
Los Alamos National Laboratory
P. O. Box 1663
Los Alamos, NM 87545

Dr. Renee B. Feldman
Los Alamos National Laboratory
P. O. Box 1663
Los Alamos, NM 87545

Dr. L. A. Ferrari
Queens College
Department of Physics
Flushing, NY 11367

Dr. C. Finfgeld
ER-542, GTN
Department of Energy
Washington, DC 20545

Dr. A. S. Fisher
Dept. of Electrical Engineering
Stanford University
Stanford, CA 94305

Dr. R. G. Fleig
Hughes Research Laboratory
3011 Malibu Canyon Road
Malibu, CA 90265

Dr. H. Fleischmann
Cornell University
Ithaca, NY 14850

Dr. E. Fontana
Dept. of Electrical Engineering
Stanford University
Stanford, CA 94305

Dr. Norval Fortson
University of Washington
Department of Physics
Seattle, WA 98195

Dr. Roger A. Freedman
Quantum Institute
University of California
Santa Barbara, CA 93106

Dr. Lazar Friedland
Dept. of Eng. & Appl. Science
Yale University
New Haven, CT 06520

Dr. Walter Friez
Air Force Avionics Laboratory
AFWAL/AADM-1
Wright/Paterson AFB, OH 45433

Dr. Shing F. Fung
Code 696
GSFC
NASA
Greenbelt, MD 20771

Dr. R. Gajewski
Div. of Advanced Energy Projects
U. S. Dept of Energy
Washington, DC 20545

Dr. H. E. Gallagher
Hughes Research Laboratory
3011 Malibu Canyon Road
Malibu, CA 90265

Dr. James J. Gallagher
Georgia Tech. EES-EOD
Baker Building
Atlanta, GA 30332

Dr. W. J. Gallagher
Boeing Aerospace Co.
P. O. Box 3999
Seattle, WA 98124

Dr. J. Gallardo
Quantum Institute
University of California
Santa Barbara, CA 93106

Dr. E. P. Garate
Dept. of Physics and Astronomy
Dartmouth College
Hanover, NH 03755

Dr. A. Garren
Lawrence Berkeley Laboratory
University of California, Berkeley
Berkeley, CA 94720

Dr. Richard L. Garwin
IBM, T. J. Watson Research Ctr.
P.O. Box 218
Yorktown Heights, NY 10598

Dr. J. Gea-Banacloche
Dept. of Physics & Astronomy
Univ. of New Mexico
800 Yale Blvd. NE
Albuquerque, NM 87131

DR. R. I. Gellert
Spectra Technology
2755 Northup Way
Bellevue, WA 98004

Dr. T. V. George
ER-531, GTN
Department of Energy
Washington, DC 20545

Dr. Edward T. Gerry, President
W. J. Schafer Associates, Inc.
1901 N. Fort Myer Drive
Arlington, VA 22209

Dr. Roy Glauber
Physics Department
Harvard University
Cambridge, MA 02138

Dr. B. B. Godfrey
Mission Research Corporation
1720 Randolph Road, S. E.
Albuquerque, NM 87106

Dr. John C. Goldstein, X-1
Los Alamos Natl. Scientific Lab.
P.O. Box 1663
Los Alamos, NM 87545

Dr. Yee Fu Goul
Plasma Physics Lab., Rm 102
S.W. Mudd
Columbia University
New York, NY 10027

Dr. C. Grabbe
Department of Physics
University of Iowa
Iowa City, Iowa 52242

Dr. V. L. Granatstein
Dept. of Electrical Engineering
University of Maryland
College Park, MD 20742

Dr. D. D. Gregoire
Quantum Institute and Dept. of Physics
University of California
Santa Barbara, CA 93106

Dr. Y. Greenzweig
Quantum Inst. and Dept. of Physics
University of California
Santa Barbara, CA 93106

Dr. Morgan K. Grover
R&D Associates
P. O. Box 9695
4640 Admiralty Highway
Marina Del Rey, CA 90291

Dr. A. H. Guenter
Air Force Weapons Laboratory
Kirtland AFB, NM 87117

Dr. K. Das Gupta
Physics Department
Texas Tech University
Lubbock, TX 79409

Dr. Benjamin Haberman
Associate Director, OSTP
Room 476, Old Exe. Office Bldg.
Washington, D.C. 20506

Dr. R. F. Hagland, Jr.
Director, Vanderbilt University
Nashville, TN 37235

34

Dr. S. F. Jacobs
Optical Sciences Center
University of Arizona
Tucson, AZ 85721

Dr. Pravin C. Jain
Asst. for Communications Tech.
Defense Communications Agency
Washington, DC 20305

Dr. E. T. Jaynes
Physics Department
Washington University
St. Louis, MO 63130

Dr. B. Carol Johnson
Ctr. for Radiation Research
National Bureau of Standards
Gaithersburg, MD 20899

Dr. Bernadette Johnson
Lincoln Laboratory
Lexington, MA 02173

Dr. Richard Johnson
Physics International
2700 Merced St.
San Leandro, CA 94577

Dr. G. L. Johnston
NW 16-232
Mass. Institute of Tech.
Cambridge, MA 02139

Dr. Shayne Johnston
Physics Department
Jackson State University
Jackson, MS 39217

Dr. William Jones
U. S. Army SDC
P. O. Box 1500
Huntsville, Al 35807-3801

Dr. R. A. Jong
Lawrence Livermore National Laboratory
P. O. Box 808/L626
Livermore, CA 94550

Dr. Howard Jory (3 copies)
Varian Associates, Bldg. 1
611 Hansen Way
Palo Alto, CA 94303

Dr. C. Joshi
University of California
Los Angeles, CA 90024

Dr. Paul Kennedy
Rockwell International/Rocketdyne Div.
6633 Canoga Avenue, FA-40
Canoga Park, CA 91304

Dr. R. Kennedy
Boeing Aerospace Company
P.O. Box 3999
Seattle, WA 98124

Dr. K. J. Kim, MS-101
Lawrence Berkeley Lab.
Rm. 223, B-80
Berkeley, CA 94720

Dr. I. Kimel
Quantum Institute
University of California
Santa Barbara, CA 93106

Dr. Brian Kincaid
AT&T Bell Labs
700 Mountain Ave.
Murray Hill, NJ 07974

Dr. S. P. Kno
Polytechnic Institute of NY
Route 110
Farmingdale, NY 11735

Dr. Xu Knogyi
Room 36-285
Mass. Institute of Technology
Cambridge MA 02139

Dr. A. Kolb
Maxwell Laboratories, Inc.
8835 Balboa Avenue
San Diego, CA 92123

Dr. Eugene Kopf
Principal Deputy Assistant
Secretary of the Air Force (RD&L)
Room 4E964, The Pentagon
Washington, D.C. 20330

Dr. P. Korn
Maxwell Laboratories, INc.
8835 Balboa Avenue
San Diego, CA 92123

Dr. S. Krinsky
Nat. Synchrotron Light Source
Brookhaven National Laboratory
Upton, NY 11973

Prof. N. M. Kroll
Department of Physics
B-019, UCSD
La Jolla, CA 92093

Dr. Thomas Kwan
Los Alamos National Scientific
Laboratory, MS608
P. O. Box 1663
Los Alamos, NM 87545

Dr. Jean Labacqz
Stanford University
SLAC
Stanford, CA 94305

Dr. Ross H. Labbe
Rockwell International/Rocketdyne Div.
6633 Canoga Avenue, FA-40
Canoga Park, CA 91304

Dr. Willis Lamb
Optical Sciences Center
University of Arizona
Tucson, AZ 87521

Dr. H. Lancaster
Lawrence Berkeley Laboratory
University of California, Berkeley
Berkeley, CA 94720

Dr. D. J. Larson
The Inst. for Accelerator Physics
Department of Physics
University of Wisconsin-Madison
Madison, WI 53706

Dr. J. LaSala
Physics Dept.
U. S. M. A.
West Point, NY 10996

Dr. Bernard Laskowski
M.S. 230-3
NASA-Ames
Moffett Field, CA 94305

Dr. Charles J. Lasnier
TRW
High Energy Physics Lab.
Stanford University
Stanford, CA 94305

Dr. Michael Lavan
U.S. Army Strategic Def. Command
ATTN: Code CSSD-H-D
P. O. Box 1500
Huntsville, AL 35807-3801

Dr. Ray Leadabrand
SRI International
333 Ravenswood Avenue
Menlo Park, CA 94025

Dr. Kotik K. Lee
Perkin-Elmer
Optical Group
100 Wooster Heights Road
Danbury, CT 06810

Dr. K. Lee
Los Alamos Nat. Scientific Lab.
Attn: X-1 MS-E531
P. O. Box 1663
Los Alamos, NM 87545

Dr. Barry Leven
NISC/Code 20
4301 Suitland Road
Washington, D.C. 20390

Dr. B. Levush
University of Maryland
College Park, MD 20742

Dr. Lewis Licht
Department of Physics
Box 4348
U. of Illinois at Chicago Cir.
Chicago, IL 60680

Dr. M. A. Lieberman
Dept. EECS
Univ. of Cal. at Berkeley
Berkeley, CA 94720

Dr. Anthony T. Lin
Dept. of Physics
University of California
Los Angeles, CA 90024

Dr. B. A. Lippmann
Stanford Linear Accel. Center
BIN 26
Stanford, CA 94305

Dr. R. Lohsen
Los Alamos National Laboratory
P. O. Box 1663
Los Alamos, NM 87545

Dr. D. D. Lowenthal
Spectra Technology
2755 Northup Way
Bellevue, WA 98004

Dr. A. Luccio
Brookhaven National Laboratory
Accelerator Dept.
Upton, NY 11973

Dr. A. Lumpkin
Los Alamos National Laboratory
P. O. Box 1663
Los Alamos, NM 87545

Dr. Phil Mace
W. J. Shafer Assoc.,Inc.
1901 N. Fort Myer Drive
Arlington, VA 22209

Dr. John Madey
S.P.R.C.
Physics Department
Stanford University
Stanford, CA 94305

Dr. Siva A. Mani
Science Applications Intl. Corp.
1040 Waltham Street
Lexington, MA 02173-8027

Dr. J. Mark
Lawrence Livermore National Lab.
Attn: L-477
P. O. Box 808
Livermore, CA 94550

Dr. T. C. Marshall
Applied Physics Department
Columbia University
New York, NY 10027

Dr. Xavier K. Maruyama
Dept. of Physics
Naval Postgraduate School
Monterey, CA 93943

Dr. Neville Marzwell
Jet Propulsion Lab.
MS 198-330
4800 Oak Grove Drive
Pasadena, CA 91109

Dr. A. Maschke
TRW
Mail Stop 01-1010
1 Space Park
Redondo Beach CA 90278

Dr. Joseph Mathew
Sachs/Freeman Associate
Landover, MD 20784

Dr. K. Matsuda
GA Technologies Inc.
P.O. Box 85608
San Diego, CA 92138

Dr. John McAdoo
Mission Research Corporation
5503 Cherokee Ave., Suite 201
Alexandria, Va 22312

Dr. D. B. McDermott
Electrical Engineering Dept.
University of California
Los Angeles, CA 90024

Dr. J. K. McIver
Dept. of Physics & Astronomy
Univ. of New Mexico
800 Yale Blvd. NE
Albuquerque, NM 87131

Dr. C. McKinstrie
MS B258
P.O. Box 1663
Los Alamos, NM 87545

Col J. F. McNulty
Ground Based Laser Proj. Office
DASD-H-F
White Sands Missile Range, NM 88002-1198

Dr. B. McVey
Los Alamos National Laboratory
P. O. Box 1663
Los Alamos, NM 87545

Dr. John Meson
DARPA
1400 Wilson Boulevard
Arlington, VA 22209

38

Col Thomas Meyer
DARPA/STO
1400 Wilson Boulevard
Arlington, VA 22209

Dr. F. E. Mills
Fermilab
P.O., Box 500
Batavia, IL 60510

Dr. D. R. Mize
Hughes Research Laboratory
3011 Malibu Canyon Road
Malibu, CA 90265

Dr. Mel Month
Brookhaven National Laboratories
Associated Universities, Inc.
Upton, L.I., NY 11973

Dr. B. N. Moore
Austin Research Assoc.
1901 Rutland Dr.
Austin, TX 78758

Dr. Gerald T. Moore
University of New Mexico
Albuquerque, NM 87131

Dr. Warren Mori
1-130 Knudsen Hall
U.C.L.A.
Los Angeles, CA 90024

Dr. Philip Morton
Stanford Linear Accelerator Center
P.O. Box 4349
Stanford, CA 94305

Dr. Jesper Munch
TRW
One Space Park
Redondo Beach, CA 90278

Dr. James S. Murphy
National Synchrotron Light Source
Brookhaven National Laboratory
Upton, NY 11975

Dr. J. Nation
Cornell University
Ithaca. NY 14850

Dr. R. Neighbours
Physics Department
Naval Postgraduate School
Monterey, CA 93943

Dr. George Neil
TRW
One Space Park
Redondo Beach, CA 90278

Dr. Kelvin Neil
Lawrence Livermore National Lab.
Code L-321, P.O. Box 808
Livermore, CA 94550

Dr. W. M. Nevins
L-639
Lawrence Livermore National Laboratory
P. O. Box 808
Livermore, CA 94550

Dr. Brian Newnam
MSJ 564
Los Alamos National Scientific Lab.
P.O. Box 1663
Los Alamos, NM 87545

Dr. W. Nexsen
Lawrence Livermore National Laboratory
P. O. Box 808
Livermore, CA 94550

Lt. Rich Nielson/ESD/INK
Hanscomb Air Force Base
Stop 21, MA 01731

Dr. Milton L. Noble (2 copies)
General Electric Company
G. E. Electric Park
Syracuse, NY 13201

Dr. K. O'Brien
Div. 1241 SNLA
Albuquerque, NM 87185

Dr. John D. O'Keefe
TRW
One Space Park
Redondo Beach, CA 90278

Dr. T. Orzechowski
L-436
Lawrence Livermore National Lab.
P. O. Box 808
Livermore, CA 94550

39

Prof. E. Ott (2 copies)
Department of Physics
University of Maryland
College Park, MD 20742

OUSDRE (R&AT)
Room 3D1067, The Pentagon
Washington, D.C. 20301

Dr. A. J. Palmer
Hughes Research Laboratory
3011 Malibu Canyon Road
Malibu, CA 90265

Dr. Robert B. Palmer
Brookhaven National Laboratories
Associated Universities, Inc.
Upton, L.I., NY 11973

Dr. J. Palmer
Hughes Research Laboratory
Malibu, CA 90265

Dr. Richard H. Pantell
Stanford University
Stanford, CA 94305

Dr. Dennis Papadopoulos
Astronomy Department·
University of Maryland
College Park, Md. 20742

Dr. P. Parks
GA Technologies
P.O. Box 85608
San Diego, Ca 92138

Dr. John A. Pasour
Mission Research Laboratory
5503 Cherokee Avenue
Alexandria, VA

Dr. C. K. N. Patel
Bell Laboratories
Murray Hill, NJ 07974

Dr. Richard M. Patrick
AVCO Everett Research Lab., Inc.
2335 Revere Beach Parkway
Everett, MA 02149

Dr. Claudio Pellegrini
Brookhaven National Laboratory
Associated Universities, Inc.
Upton, L.I., NY 11973

Dr. Samuel Penner
Center for Radiation Research
National Bureau of Standards
Gaithersburg, MD 20899

Dr. D. E. Pershing
Mission Research Corporation
5503 Cherokee Avenue
Alexandria, VA 22312

Dr. J. M. Peterson
Lawrence Berkeley Laboratory
University of California, Berkeley
Berkeley, CA 94720

Dr. M. Piestrup
Adelphi Technology
13800 Skyline Blvd. No. 2
Woodside, CA 94062 CA 94305

Dr. Alan Pike
DARPA
1400 Wilson Boulevard
Arlington, VA 22209

Dr. Hersch Pilloff
Code 421
Office of Naval Research
Arlington, VA 22217

Dr. A. L. Pindroh
Spectra Technology
2755 Northup Way
Bellevue, WA 98004

Dr. D. J. Pistoresi
Boeing Aerospace Company
P. O. Box 3999
Seattle, WA 98124-2499

Dr. Peter Politzer
General Atomic Tech., Rm. 13/260
P. O. Box 85608
San Diego, CA 92138

Major Donald Ponikvar
U. S. Army SDC
P. O. Box 15280
Arlington, VA 22245-0280

Dr. S. E. Poor
Lawrence Livermore National Laboratory
P. O. Box 808
Livermore, CA 94550

40

Dr. J. B. Rosenzweig
The Inst. for Accelerator Physics
Department of Physics
University of Wisconsin-Madison
Madison, WI 53706

Dr. J. Ross
Spectra Technology
2755 Northup Way
Bellevue, WA 98004

Dr. N. Rostoker
University of California
Department of Physics
Irvine, CA 92717

Dr. G. A. Saenz
Hughes Research Laboratory
3011 Malibu Canyon Road
Malibu, CA 90265

Dr. Antonio Sanchez
Lincoln Laboratory
Mass. Institute of Tech.
Room B213
P. O. Box 73
Lexington, MA 02173

Dr. Aldric Saucier
BMD-PO
Ballistic Missile Defense
Program Office
P. O. Box 15280
Arlington, VA 22215

Dr. A. Saxman
Los Alamos National Scientific Lab.
P. O. Box 1663, MSE523
Los Alamos, NM 87545

Dr. J. Scharer
ECE Dept.
Univ. of Wisconsin
Madison, WI 53706

Dr. E. T. Scharlemann
L626
Lawrence Livermore National Laboratory
P. O. Box 808
Livermore, CA 94550

Prof. S. P. Schlesinger
Dept. of Electrical Engineering
Columbia University
New York, NY 10027

Dr. Howard Schlossberg
AFOSR
Bolling AFB
Washington, D.C. 20332

Dr. George Schmidt
Stevens Institute of Technology
Physics Department
Hoboken, NJ 07030

Dr. M. J. Schmitt
Los Alamos National Laboratory
P. O. Box 1663
Los Alamos, NM 87545

Dr. Stanley Schneider
Rotodyne Corporation
26628 Fond Du Lac Road
Palos Verdes Peninsula, CA 90274

Dr. N. Schoen
TRW DSSG
One Space Park
Redondo Beach, CA 90278

Dr. M. L. Scott
Los Alamos National Laboratory
P. O. Box 1663
Los Alamos, NM 87545

Dr. Richard L. Schriever (DP-23)
Director, Office of Inertial Fusion
U. S. Department of Energy
Washington, D.C. 20545

Dr. R. W. Schumacher
Hughes Research Laboratories
3011 Malibu Canyon Road
Malibu, CA 09265

Dr. H. Schwettmann
Phys. Dept. & High Energy
Physics Laboratory
Stanford University
Stanford, CA 94305

Dr. Marlan O. Scully
Dept. of Physics & Astronomy
Univ. of New Mexico
800 Yale Blvd. NE
Albuquerque, NM 87131

Dr. S. B. Segall
KMS Fusion
3941 Research Park Dr.
P.O. Box 1567
Ann Arbor, MI 48106

Dr. Robert Sepucha
DARPA
1400 Wilson Boulevard
Arlington, VA 22209

Prof. P. Serafim
Northeastern University
Boston, MA 02115

Dr. A. M. Sessler
Lawrence Berkeley Laboratroy
University of California
1 Cyclotron Road
Berkeley, CA 94720

Dr. W. Sharp
L-626
Lawrence Livermore National Laboratory
P. O. Box 808
Livermore, CA 94550

Dr. Earl D. Shaw
Bell Laboratories
600 Mountain Avenue
Murray Hill, NJ 07974

Dr. J. P. Sheerim
KMS Fusion
P.O. Box 1567
Ann Arbor, MI 48106

Dr. R. Shefer
Science Research Laboratory
15 Ward Street
Somerville, MA 02143

Dr. R. L. Sheffield
Los Alamos National Laboratory
P.O. Box 1663
Los Alamos, NM 87545

Dr. Shemwall
Spectra Technology
2755 Northup Way
Bellevue, WA 98004

Dr. Shen Shey
DARPA/DEO
1400 Wilson Boulevard
Arlington, VA 22209

Dr. D. Shoffstall
Boeing Aerospace Company
P.O. Box 3999
Seattle, WA 98124

Dr. I. Shokair
SNLA, Org. 1271
Albuquerque, NM 87185

Dr. J. S. Silverstein
Harry Diamond Laboratories
2800 Powder Mill Road.
Adelphi, MD 20783

Dr. Jack Slater
Spectra Technology
2755 Northup Way
Bellevue, WA 98004

Dr. Kenneth Smith
Physical Dynamics, Inc.
P.O. Box 556
La Jolla, CA 92038

Dr. Lloyd Smith
Lawrence Berkeley Laboratory
University of California
1 Cyclotron Road
Berkeley, CA 94720

Dr. Stephen J. Smith
JILA
Boulder, CO 80302

Dr. T. Smith
TRW, Inc.
One Apace Park
Redondo Beach, CA 90278 R1/2044

Dr. Todd Smith
Hansen Labs
Stanford University
Stanford, CA 94305

Dr. Joel A. Snow, M.S. E084
Senior Technical Advisor
Office of Energy Research
U. S. Department of Energy
Washington, D.C. 20585

Dr. J. Z. Soln (22300)
Harry Diamond Laboratories
2800 Powder Mill Road
Adelphi. MD 20783

Dr. G. Spalek
Los Alamos National Laboratory
P. O. Box 1663
Los Alamos, NM 87545

Dr. Richard Spitzer
Stanford Linear Accelerator Center
P.O. Box 4347
Stanford, CA 94305

Mrs. Alma Spring
DARPA/Administration
1400 Wilson Boulevard
Arlington, VA 22209

SRI/MP Reports Area G037 (2 copies)
ATTN: D. Leitner
333 Ravenswood Avenue
Menlo Park, CA 94025

Dr. W. Stein
Los Alamos National Laboratory
P. O. Box 1663
Los Alamos, NM 8754~

Dr. L. Steinhauer
STI
2755 Northup Way
Bellevue, WA 98004·

Dr. Efrem J. Sternbach
Lawrence Berkeley Laboratory
University of California, Berkeley
Berkeley, CA 94720

Dr. M. Strauss
Department of Physics
University of California at Irvine
Irvine, CA 92717

Dr. W. C. Stwalley
Iowa Laser Facility
University of Iowa
Iowa City, Iowa

Dr. R. Sudan
Lab. of Plasma Studies
Cornell University
Ithaca, NY 14850

Dr. P. W. Sumner
Hughes Research Laboratory
3011 Malibu Canyon Road
Malibu, CA 90265

Dr. David F. Sutter
ER 224, GTN
Department of Energy
Washington, D.C. 20545

Dr. Abraham Szoke
ML/L-470
Lawrence Livermore Natl. Lab.
P.O. Box 808
Livermore, CA 94550

Dr. R. Taber
Dept. of Phys. & High Energy Lab.
Stanford University
Stanford, CA 94305

Dr. T. Tajima
IFS
Univ. of Texas
Austin, TX 78712

Dr. H. Takeda
Los Alamos National Laboratory
P. O. Box 1663
Los Alamos, NM 87545

Dr. J. J. Tancredi
Hughes Aircraft Co.
Electron Dynamics Division
3100 West Lomita Blvd.
Torrance, CA 90509

Dr. Milan Tekula
AVCO Everett Research Lab.
2385 Revere Beach Parkway
Everett, MA 02149

Dr. R. Temkin (2 copies)
Mass. Institute of Technology
Plasma Fusion Center
Cambridge, MA 02139

Dr. L. Thode
Los Alamos National Laboratory
P. O. Box 1663
Los Alamos, NM 87545

Dr. Keith Thomassen, L-637
Lawrence Livermore National Laboratory
P. O. Box 808
Livermore, CA 94550

Dr. Harold Thompson
TRW, Inc.
R1/2120
One Space Park
Redondo Beach, Ca 90278

Dr. Norman H. Tolk
Physics Department
Vanderbilt University
Nashville, TN 37240

Dr. Kang Tsang
Science Applications Intl. Corp.
10260 Campus Point Drive
San Diego, CA 92121

Dr. E. Tyson
Boeing Aerospace Company
P.O. Box 3999
Seattle, WA 98124

Dr. H. S. Uhm
Naval Surface Warfare Center
White Oak Lab.
Silver Spring, MD 20903-5000

Dr. L. Ulstrup
TRW, Inc.
One Space Park
Redondo Beach, Ca 90278

Under Secretary of Defense (R&E)
Office of the Secretary of Defense
Room 3E1006, The Pentagon
Washington, D.C. 20301

Dr. L. Vahala
Physics Dept.
College of William & Mary
Williamsburg, VA 23185

Dr. A. Valla
Spectra Technology
2755 Northup Way
Bellevue, WA 98004

Dr. A. Vetter
Boeing Aerospace Company
P.O. Box 3999
Seattle, WA 98124

Dr. A. A. Vetter
Spectra Technology
2755 Northup Way
Bellevue, WA 98004

Dr. G. Vignola
Brookhaven National Laboratories
Associated Universities, Inc.
Upton, L.I., NY 11973

Dr. S. A. Von Laven
KMS Fusion Inc.
Ann Arbor, MI 48106

Dr. John E. Walsh
Wilder Laboratory
Department of Physics (HB 6127)
Dartmouth College
Hanover NH 03755

Dr. W. M. Walsh, Jr.
Bell Laboratories
600 Mountain Avenue
Room 1-D 332
Murray Hill, NJ 07974

Dr. Jiunn-Ming Wang
Brookhaven National Laboratories
Associated Universities, Inc.
Upton, L.I., NY 11973

Dr. T-S. Wang
Los Alamos National Laboratory
P. O. Box 1663
Los Alamos, NM 87545

Dr. J. F. Ward
University of Michigan
Ann Arbor, MI 48109

Dr. E. Warden
Code PDE 106-3113
Naval Electronics Systems Command
Washington, DC 20363

Dr. Roger W. Warren
Los Alamos National Sciencific Lab.
P.O. Box 1663
Los Alamos, NM 87545

Dr. J. Watson
Los Alamos National Laboratory
P. O. Box 1663
Los Alamos, NM 87545

Dr. B. Weber
Harry Diamond Laboratories
2800 Powder Mill Road
Adelphi, MD 20783

Dr. Lee Webster
BMD/ATC
Box 1500
Huntsville, AL 35807

Dr. J. T. Weir
Lawrence Livermore National Laboratory
P. O. Box 808
Livermore, CA 94550

Dr. R. Whitefield
15260 Dickens Ave.
San Jose, CA 95124

Ms. Bettie Wilcox
Lawrence Livermore National Lab.
ATTN: Tech. Info. Dept. L-3
P.O. Box 808
Livermore, CA 94550

Dr. Mark Wilson
National Bureau of Standards
Bldg. 245, Rm. B-119
Gaithersburg, MD 20899

Dr. H. Winick
Stanford Synch Rad. Lab.
SLAC Bin 69
P.O. Box 44349
Stanford, CA 94550

Dr. J. Workman
Berkeley Research Associates
P.O. Box 241
Berkeley, CA 94701

Dr. Jack Wong (L-71)
Lawrence Livermore National Lab.
P. O. Box 808
Livermore, CA 94550

Dr. Thomas P. Wright
Sandia National Laboratories
ORG. 1231, P.O. Box 5800
Albuquerque, NM 87185

Dr. J. Wurtele
M.I.T.
NW 16-234
Plasma Fusion Center
Cambridge, MA 02139

Dr. Ming Xie
Dept. of Physics
Stanford University
Stanford, CA 94305

Dr. Yi-Ton Yan
MS-B259
Los Alamos National Lab.
Los Alamos, NM 87545

Dr. A. Yariv
California Institute of Tech.
Pasadena, CA 91125

Dr. F. G. Yee
Columbia University
New York, NY 10027

Dr. J. Yeh
Allied Corporation
31717 La Tienda Dr.
Westlake Village, CA 91362

Dr. A. Yeremian
Boeing Aerospace Company
P.O. Box 3999
Seattle, WA 98124

Dr. Barbara Yoou
R & D Associates
1401 Wilson Blvd., Suite 500
Arlington, VA 22209

Dr. Li Hua Yu
725B, NSLS
Brookhaven National Laboratory
Upton, NY 11973

Dr. Simon S. Yu
Lawrence Livermore National Laboratory
P. O. Box 808
Livermore, CA 94550

Dr. Mark Zedikev
103 S. Goodwin
Urbana, IL 61801

Dr. M. S. Zisman
Lawrence Berkeley Laboratory
University of California, Berkeley
Berkeley, CA 94720

Dr. J. Zumdieck
Spectra Technology
2755 Northup Way
Bellevue, WA 98004

Records   1 copy